Characterization of the Backbone Dynamics of Folded and Denatured States of an SH3 Domain†

Neil A. Farrow,‡ Ouwen Zhang,‡,§ Julie D. Forman-Kay,§,|| and Lewis E. Kay*,‡

Protein Engineering Network Centres of Excellence and Departments of Medical Genetics, Biochemistry and Chemistry, University of Toronto, Toronto, Ontario M5S 1A8, Canada, Biochemistry Research Division, Hospital for Sick Children, 555 University Avenue, Toronto, Ontario M5G 1X8, Canada

Received October 10, 1996; Revised Manuscript Received December 2, 1996⊗

ABSTRACT: Measurements of ^{15}N NMR relaxation parameters have been used to characterize the backbone dynamics of folded and denatured states of the N-terminal SH3 domain from the adapter protein drk, in high salt or guanidinium chloride, respectively. Values of the spectral density function evaluated at a number of frequencies are compared. The levels of backbone dynamics in the folded protein show little variation across the molecule and are of similar magnitude to those determined previously for the folded state of the protein in exchange with an unfolded state at low salt concentrations [Farrow et al. (1995) *Biochemistry 34*, 868−878]. The denatured state of the domain exhibits both more extensive and more heterogeneous dynamics than the folded state. In particular the profile of the spectral density function evaluated at zero-frequency for the unfolded state of the domain indicates that residues in the middle of the protein sequence are considerably less mobile than those at the termini. These data suggest that the molecule is not behaving as an extended polymer and that concerted motions of the central portions of the molecule are occurring, consistent with a reasonably compact conformation in this region. The backbone dynamics of the folded and unfolded states were studied at two temperatures. The level of high-frequency motions in the folded molecule is largely unaffected by changes in temperature, whereas an increase in temperature results in increased high-frequency motion in the unfolded state.

Understanding the processes that enable proteins to adopt stable, folded conformations has been the subject of a great deal of research over many years. While the native states of proteins—the end points of folding processes—have been characterized extensively, relatively little is known about the nature of folding intermediates and the unfolded states of proteins. In order to fully understand folding pathways a more complete description of these states will be required. Consequently a significant amount of effort has been devoted to obtaining such information. Nuclear magnetic resonance (NMR)[1] studies have been performed to characterize the regions of persistent structure in a growing number of unfolded and partly unfolded structures (Neri et al., 1992; Alexandrescu et al., 1994; Feng et al., 1994; Logan et al., 1994; Redfield et al., 1994; Arcus et al., 1995; Buck et al., 1995). While the results of these investigations suggest some preferential sampling of conformational space, most biophysical studies [extensively reviewed elsewhere, see Dobson (1992) and Shortle (1993)] indicate that reference to a single unfolded state is an oversimplification and that unfolded proteins sample a continuum of conformational states.

Many studies of the unfolded states of proteins have focused on establishing the amount of residual structure present. However, the fact that unfolded proteins are likely to rapidly sample a number of alternative conformations indicates that these states must be highly mobile. Thus, in order to fully characterize the unfolded state of a protein it will be necessary to determine the extent and time scales of these motions. Heteronuclear NMR relaxation studies, which have been widely applied to determine the backbone dynamics of folded proteins, also permit extensive characterization of the dynamics of unfolded states of proteins. A number of such relaxation studies have now been reported for a range of proteins containing differing amounts of residual structure (Torchia et al., 1975; van Mierlo et al., 1993; Alexandrescu & Shortle, 1994; Logan et al., 1994; Redfield et al., 1994; Farrow et al., 1995a; Frank et al., 1995; Buck et al., 1996). Many of these relaxation studies are reported in conjunction with structural information, and it appears that the levels of internal motion within the unfolded states are closely related to the nature and extent of the residual structure within the protein. However, despite the insight provided by previous studies, the relationship between residual structure and the internal dynamics of unfolded states of proteins remains

† This work was supported through grants from the Natural Sciences and Engineering Research Council of Canada (L.E.K.), the Medical Research Council of Canada (J.D.F.), and the National Cancer Institute of Canada (J.D.F. and L.E.K.) with funds from the Canadian Cancer Society. N.A.F. is a Research Fellow of the National Cancer Institute of Canada supported with funds provided by the Canadian Cancer Society. O.Z. acknowledges a graduate fellowship from the University of Toronto.

* Corresponding author.

‡ Protein Engineering Network Centres of Excellence and Departments of Medical Genetics, Biochemistry and Chemistry, University of Toronto.

§ Hospital for Sick Children.

|| Department of Biochemistry, University of Toronto.

⊗ Abstract published in *Advance ACS Abstracts,* February 1, 1997.

[1] Abbreviations: 3D, three-dimensional; T_1, longitudinal relaxation time; T_2, transverse relaxation time; NOE, nuclear Overhauser effect; ω_H, proton Larmor frequency; ω_N, nitrogen Larmor frequency; SH3, Src homology 3; drkN SH3, N-terminal SH3 domain of drk; NMR, nuclear magnetic resonance; F_S, fully stabilized folded state of the drkN SH3 domain in 0.4 M Na_2SO_4; F_{exch}, folded state of the drkN SH3 domain existing in equilibrium with an unfolded state in low ionic strength aqueous buffer; U_{Gdn}, denatured state of the drkN SH3 domain in 2 M guanidinium chloride; U_{exch}, unfolded state of the drkN SH3 domain existing in equilibrium with a folded state in low ionic strength aqueous buffer; TFE, trifluoroethanol; ACTH, adrenocorticotropic hormone.

S0006-2960(96)02548-2 CCC: $14.00

poorly understood, principally as a result of the small number of systems that have currently been characterized.

Src homology 3 (SH3) domains are found in many proteins involved in cellular signaling pathways. These domains mediate interactions between proteins in signaling cascades via sequence specific binding to proline rich regions in other target proteins [for review see Pawson (1995)]. The N-terminal SH3 domain of the *Drosophila* adapter protein drk (drkN SH3) provides an excellent model for studying the process of protein folding. While many other isolated SH3 domains form stable folded structures in solution, the drkN SH3 domain exists in an equilibrium between a folded (F_{exch}) and an unfolded (U_{exch}) state, at near-neutral pH in aqueous buffer (Zhang & Forman-Kay, 1995), with an exchange rate of roughly 1 per second (Farrow et al., 1995a). A similar equilibrium between folded an unfolded states was reported for the N-terminal SH3 domain of Grb2, the mammalian homologue of drk (Goudreau et al., 1994). There is additional evidence to suggest that isolated SH3 domains are not uniformly stable. For example, the SH3 domain of Src exhibits fewer NOEs than expected (relative to other SH3 domains) and has high amide proton exchange rates throughout the protein (Yu et al., 1992), suggestive of unstable secondary structure. Interestingly, an equilibrium between folded and unfolded states was not observed in two NMR studies of the N-terminal Grb2 SH3 domain bound to a proline-rich peptide (Wittekind et al., 1994; Teresawa et al., 1994), consistent with stabilization of the folded state upon binding.

The low stability of isolated SH3 domains may result from the loss of stabilizing interactions with other domains within the intact protein or with other proteins. The structure of the intact mammalian homologue of drk, Grb2, was recently published (Maignan et al., 1995). In the absence of the proline-rich ligand and in the crystal state the protein adopts a dimeric conformation with contacts between the C-terminal SH3 domain of one molecule and the SH2 domain and C-terminal SH3 domain of the other. Additionally, a small region of interaction between the N- and C-terminal SH3 domains of each subunit was observed. More recently however, NMR studies of both the intact molecule as well as isolated fragments comprising individual SH2 and SH3 domains indicate that in solution the subunits are independent (Yuzawa et al., 1996). It has been observed in vivo that drk is constitutively associated with the protein Sos (Schlessinger, 1993), and this interaction may well serve to stabilize the folded state of the protein. This model is supported by calorimetric studies of the C-terminal SH3 domain of Sem5 (Lim et al., 1994) where it was demonstrated that the protein was maximally stable at pH 4.7, suggesting that electrostatic interactions amongst a number of acidic residues may destabilize the domain at neutral pH. It is of interest to note that these acidic residues contact the arginine-rich regions flanking poly-proline helices of target molecules, thus stabilizing the complex.

NMR structural studies have been performed to characterize both the F_{exch} and U_{exch} states of the drkN SH3 domain (Zhang & Forman-Kay, 1995; Zhang et al., 1994, 1996). This work has demonstrated that the equilibrium may be driven to either a stable folded (F_S) or fully unfolded state (U_{Gdn}) by an increase in salt concentration or addition of denaturant, respectively. In a previous paper we have also determined the backbone dynamics of the drkN SH3 domain in the exchanging folded−unfolded system (Farrow et al., 1995a). The results showed that the levels of dynamics in the F_{exch} state of the domain were typical of those seen in other folded proteins. In contrast, the levels of internal dynamics of the U_{exch} state of the protein were more extensive and more heterogeneous than those typically associated with folded proteins, while still being consistent with the adoption of a relatively compact conformation in solution. The work presented here serves to significantly expand upon the results obtained for the exchanging folded−unfolded system by describing the backbone dynamics of the F_S and U_{Gdn} states of the domain. By studying the two states of the protein in isolation the number of residues for which the dynamics may be obtained is increased significantly. Additionally, the results of the current study permit comparison of the backbone dynamics of the exchanging (F_{exch}, U_{exch}) states with those of the fully folded and denatured states of the protein.

MATERIALS AND METHODS

Protein Preparation. Samples of ^{15}N-labeled drkN SH3 domain were prepared as described previously (Zhang & Forman-Kay, 1995). Fully folded and denatured samples of the drkN SH3 domain were prepared in buffers containing 0.4 M Na_2SO_4 and 2.0 M guanidinium chloride, respectively. Both buffers also contained 0.05 M sodium phosphate, 90% H_2O/10% D_2O, pH 6, and the protein concentration in both samples was 1 mM.

NMR Spectroscopy. NMR spectra were collected at 500 MHz on a Varian Unity spectrometer and at 600 MHz on a Varian Unity Plus spectrometer. Both spectrometers were equipped with triple resonance pulsed field gradient probes with actively shielded *z*-gradients. Measurements were made at 14 and 30 °C. The pulse sequences that were used to determine the ^{15}N T_1 and T_2 relaxation times and values of the steady-state ^{1}H−^{15}N NOE have been described previously (Farrow et al., 1994). All the pulse sequences employed enhanced sensitivity pulsed field gradient techniques and utilized water-selective shaped pulses to minimize solvent dephasing (Grzesiek & Bax, 1993). Spectra recorded at 500 MHz were collected as 160 × 512 complex matrices with sweep widths of 1500 and 8000 Hz in the ^{15}N and ^{1}H dimensions, respectively. Spectra collected at 600 MHz were acquired as 160 × 640 matrices with sweep widths of 1500 and 10000 Hz in the ^{15}N and ^{1}H dimensions, respectively. Values of T_1 were determined from seven spectra recorded with delays ranging from 0.011 to 0.899 s, with 32 scans per t_1 point and with a 1 s recycle delay. Concerns about heating during the CPMG period, as a result of the high concentrations of Na_2SO_4 and guanidinium chloride in samples of the folded and unfolded SH3 domains, respectively, led us to employ longer recycle delays when collecting T_2 spectra. Spectra for the measurement of transverse relaxation times of the unfolded sample were recorded with a recycle delay of 3 s and 8 scans per t_1 point while spectra acquired for the folded sample were collected with a 2 s recycle delay and with 16 scans per t_1 point. Each T_2 series was composed of eight time points with delays between 0.016 and 0.187 s. Values of the steady-state NOE were determined from pairs of spectra, recorded with and without proton saturation. Proton saturation was achieved by the application of ^{1}H 120° pulses every 5 ms (Markley et al., 1971). Spectra recorded with proton saturation utilized a 5 s recycle delay followed by a 3 s period of saturation, while

spectra recorded in the absence of saturation employed a recycle delay of 8 s. All data were processed using the nmrPipe system of software (Delaglio et al., 1995), and peak volumes were obtained using the surface fitting routines in nmrPipe.

Data Analysis. Values of T_1 and T_2 were determined by fitting the measured peak volumes to a single exponential decay curve, and uncertainties in the relaxation times were determined from Monte Carlo simulations (Press et al., 1986; Kamath & Shriver, 1989; Palmer et al., 1991). Values of the steady-state NOE were established from the ratio of peak intensities obtained from spectra recorded with and without proton saturation. For the unfolded state of the protein three pairs of spectra were collected for each temperature and field strength, and the value of the steady-state NOE was calculated as the average ratio of the peak intensities in the presence and absence of proton saturation. The uncertainties in these values are reported as the standard deviation of the three pairs of measurements. For the folded protein, NOE spectra were collected in triplicate for a single experimental condition, (14 °C, 600 MHz). The fractional uncertainty in each of the values of the steady-state NOE obtained under these conditions was then used to estimate the error in NOE measurements obtained for the other experimental conditions, in which a single pair of spectra were recorded.

Values of the spectral density function were extracted from the measured relaxation parameters using a procedure similar to that employed in a previous analysis of the F_{exch} and U_{exch} states of the SH3 domain (Farrow et al., 1995a) and described in more detail elsewhere (Farrow et al., 1995b). Briefly, the method assumes that the spectral density function, $J(\omega)$, varies slowly with respect to frequency for $\omega \approx \omega_H$ and thus that the values of $J(\omega_H \pm \omega_N)$ may be represented using a first-order Taylor series expansion about ω_H. Under such an assumption it can be shown that the contributions to the longitudinal and transverse relaxation rates and the steady-state NOE (Abragam, 1961) from values of the spectral density function evaluated at high frequency can be simplified in the following manner (Farrow et al., 1995b):

$$1/T_1 = (d^2/4)[3J(\omega_N) + 7J(0.93\omega_H)] + c^2J(\omega_N) \quad (1)$$

$$1/T_2 = (d^2/8)[4J(0) + 3J(\omega_N) + 13J(0.96\omega_H)] + (c^2/6)[3J(\omega_N) + 4J(0)] \quad (2)$$

$$\mathrm{NOE} = 1 + (d^2/4)(\gamma_H/\gamma_N)[5J(0.86\omega_H)]T_1 \quad (3)$$

where $d = [\mu_0 h\gamma_N\gamma_H/(8\pi^2)]\langle r_{NH}^{-3}\rangle$, $c = (\omega_N/\sqrt{3})(\sigma_{||} - \sigma_\perp)$, μ_0 is the permeability of free space, h is Planck's constant, γ_H and γ_N are the proton and nitrogen gyromagnetic ratios, respectively, r_{NH} is the amide bond length, and $\sigma_{||}$ and $\sigma_\perp$ are the parallel and perpendicular components of the assumed axially symmetric chemical shift tensor. The value of $J(0.86\omega_H)$, eq 3, may be determined directly from the measured values of T_1 and NOE. Determination of the values of the spectral density function at zero-frequency and ω_N from eqs 1 and 2 first requires that the values of $J(0.93\omega_H)$ and $J(0.96\omega_H)$ in eqs 1 and 2 be estimated. A number of approaches may be used to obtain these values. However, as we have previously demonstrated (Farrow et al., 1995b), the method of estimation has a negligible influence on the accuracy to which $J(0)$ and $J(\omega_N)$ may be determined. In the work presented here the values of $J(0.93\omega_H)$ and $J(0.96\omega_H)$ in eqs 1 and 2 were obtained directly from the values of $J(0.86\omega_H)$ determined from eq 3 assuming that $J(\omega) \propto 1/\omega^2$ at $\omega \approx \omega_H$, [Method 2 in Farrow et al. (1995b)]. Uncertainties in the values of the spectral density function were determined using a Monte Carlo procedure based on the uncertainties in the measured relaxation parameters.

Determination of the value of the spectral density function at zero-frequency is complicated by the contributions that motions on a millisecond-microsecond time scale make to the transverse relaxation rate. These contributions are often included in equations describing the observed transverse relaxation rate, R_2, by an additional term, R_{ex}, such that

$$R_2 = R_{2,dd} + R_{2,csa} + R_{ex} \quad (4)$$

where $R_{2,dd}$ represents the dipole−dipole component of the relaxation and $R_{2,csa}$ is the contribution arising as a result of chemical shift anisotropy. Assuming that the contribution from the millisecond−microsecond motions scales with the square of the field strength (Carrington & McLachlan, 1967) it is possible to determine the value of R_{ex} from measurement of the relaxation parameters at two spectrometer frequencies. Thus when data are collected at both 500 and 600 MHz the values of $J(0)$ and R_{ex} may be obtained from the following expressions:

$$J(0) = (1/\beta)[\{1/T_2^{600} - \kappa 1/T_2^{500}\} - (3d^2/8)\{J(\omega_N^{600}) - \kappa J(\omega_N^{500})\} - (c_{600}^2/2)\{J(\omega_N^{600}) - J(\omega_N^{500})\} - (13d^2/8)\{J(0.96\omega_H^{600}) - \kappa J(0.96\omega_H^{500})\}] \quad (5)$$

$$R_{ex} = 1/T_2^{500} - (d^2/2 + 2c_{500}^2/3)J(0) - (3d^2/8 + c_{500}^2/2)J(\omega_N^{500}) - (13d^2/8)J(0.96\omega_H^{500}) \quad (6)$$

in which the superscripts and subscripts denote the frequency of the spectrometers, the constant d is as defined above, c_i is equivalent to the constant c defined in conjunction with eqs 1 and 2 and evaluated at spectrometer frequency i, $\kappa = (\omega_H^{600}/\omega_H^{500})^2$, and $\beta = (d^2/2)(1 - \kappa)$.

The approach described above enables the backbone dynamics of the protein to be characterized in terms of values of the spectral density function of the amide bond vectors. Such an analysis is attractive because few assumptions are required about the form of either the motion of the protein or the spectral density function itself. However, one consequence of the fact that no models of the protein dynamics are required is that the spectral density values obtained do not provide a clear picture of the internal motions present in the protein. An alternative approach is to use explicit definitions for the form of the spectral density function such as the "model-free" spectral density function of Lipari and Szabo (1982a,b) given by

$$J(\omega) = {}^2/_5\{S^2\tau_m/[1 + (\omega^2\tau_m^2)] + (1 - S^2)\tau/[1 + (\omega\tau)^2]\} \quad (7)$$

in which τ_m is the overall correlation time, S^2 is the generalized order parameter squared, τ_e is the correlation time for internal motions, and $1/\tau = 1/\tau_m + 1/\tau_e$. Model-free spectral density function based approaches and extensions thereof (Clore et al., 1990) have been used successfully to analyze the dynamics of a large number of proteins [for reviews see Palmer et al. (1993) and Wagner et al. (1993)].

The first step in performing such an analysis is the determination of the value of the overall correlation time of the protein, τ_m, for which there are a number of approaches available. Ratios of T_1/T_2 may be used directly to determine τ_m under the assumptions that transverse relaxation does not contain contributions from millisecond-microsecond time-scale motions and that $\omega\tau_e \ll 1$ (Kay et al., 1989). A more sophisticated approach utilizes a grid search in τ_m while optimizing S^2 and τ_e for each residue. It is common in both approaches to consider only residues which have T_1/T_2 ratios close to the average value for the molecule, i.e. residues for which it is assumed that the observed relaxation data may be fit using the spectral density function in eq 7. Using this optimum τ_m as a starting point, the need for extended model-free spectral density functions (Clore et al., 1991) and for the inclusion of R_{ex} terms to account for the affects of millisecond−microsecond time scale motion may then be assessed and the overall correlation time refined in an iterative manner (Stone et al., 1993; Kördel et al., 1992; Akke et al., 1993; Mandel et al., 1995).

One concern with characterizing the dynamics of an unfolded protein using the model-free spectral density function results from the requirement of an overall correlation time describing the tumbling of the entire molecule. It has been noted previously that the T_1/T_2 ratio of a partially unfolded form of BPTI (van Mierlo et al., 1993) shows a large degree of variation across the protein suggesting that the rotation of the molecule may not be adequately described by a single correlation time. As will be discussed in the results section below, the T_1/T_2 ratios of residues in the unfolded state of the drkN SH3 domain also show large variations across the protein indicating that assignment of a single correlation time for the molecule may be inappropriate. While these concerns exist for the unfolded state, analysis of the folded state is much more straightforward and we have performed a model-free-based analysis primarily to aid in the interpretation of differences between the dynamics of the F_S and F_{exch} folded states of the protein.

As described above, T_1, T_2, and steady-state $^1H-^{15}N$ NOE data were collected at both 500 and 600 MHz. Values of the model-free spectral density function parameters were determined by fitting the relaxation data collected at both 500 and 600 MHz simultaneously. Optimal values of τ_m were determined for each experimental condition by considering only the relaxation data of residues with T_1/T_2 ratios within one standard deviation of the mean value. With the above reservations about the application of this procedure to data recorded on an unfolded protein in mind we have analyzed the relaxation data from both the folded and the unfolded protein in this manner.

RESULTS

Relaxation Parameters. Due to spectral overlap relaxation data could not be collected for a number of the 57 (non-proline and non-N-terminal) residues in the protein. Values of T_1, T_2, and the steady-state $^1H-^{15}N$ NOE of the F_S state were determined for 53 residues at 30 °C and for 55 residues at 14 °C. In spite of the decreased amide−proton chemical shift dispersion associated with the U_{Gdn} state, relaxation parameters were determined for 48 residues at 30 °C and for 50 residues at 14 °C, permitting extensive characterization of the unfolded state. 2D correlation spectra corresponding to the first time points of the T_1 experiments for both the folded and unfolded states of the drkN SH3 domain are given in the Supporting Information. Figure 1 shows the values of the relaxation parameters measured at 14 °C for the F_S and U_{Gdn} states of the drkN SH3 domain at 500 and 600 MHz. Tables listing the values of T_1, T_2, and the steady-state $^1H-^{15}N$ NOE obtained for all of the different experimental conditions (i.e., temperatures of 14 and 30 °C and field strengths of 500 and 600 MHz) are supplied in the Supporting Information.

Generally, the relaxation parameters of the F_S state exhibit less variation than those of the U_{Gdn} state, an observation in agreement with our previous study of the F_{exch} and U_{exch} states of the SH3 domain. As the information about protein dynamics contained in the relaxation parameters is propagated into the calculated values of the spectral density function, differences in the levels of dynamics within and between the states of the SH3 domain are discussed in relation to the values of the spectral density function themselves.

Spectral Density Functions. This study permitted the determination of the values of the spectral density function at five frequencies: zero-frequency, the ^{15}N Larmor frequencies of 50 and 60 MHz, and the high frequencies given by 0.86 times the ^1H Larmor frequency, i.e., 430 and 516 MHz for the 500 and 600 MHz spectrometer data, respectively. Figure 2 shows the values of the spectral density function at 0, 50, and 430 MHz for both the folded and the unfolded states of the drkN SH3 domain at 14 °C. Values of the spectral density function determined at 60 and 516 MHz showed similar trends to those observed at 50 and 430 MHz, respectively. The measured values of the spectral density function for residues in the folded and unfolded states of the protein, at both temperatures considered, were always non-negative and decreased as a function of frequency. Complete tables of the values of the spectral density function under all experimental conditions are provided in the Supporting Information. In addition the spectral density function values previously obtained for both the F_{exch} and U_{exch} states of the protein (Farrow et al., 1995a) are indicated in Figure 2.

As discussed above motions on a millisecond−microsecond time scale may contribute to transverse relaxation rates and are manifest as increases in the values of the spectral density function evaluated at zero-frequency. The magnitude of these contributions has been assessed using eqs 5 and 6 above. In theory the R_{ex} contribution to transverse relaxation should always be positive; however, the values of R_{ex} that were determined in the current study were often negative, especially in the case of the folded protein. Note that values of $J(0\ \text{MHz})$ and R_{ex} were determined from the difference in the T_2 values recorded at 500 and 600 MHz. These two field strengths differ by a factor of only 1.2, and thus the differences between the two values of T_2 are relatively small. A simple treatment of the errors reveals that deriving the value of $J(0\ \text{MHz})$ from the difference in T_2 values at 500 and 600 MHz (see eq 5) leads to a roughly fourfold increase in the fractional error relative to that obtained when the value of $J(0\ \text{MHz})$ is derived from data at a single field strength. Moreover, small R_{ex} contributions can not be measured accurately using an approach based on data recorded at two similar field strengths. In principle, other methods such as CPMG-based T_2 measurements where the delay between successive 180° pulses is varied in a series of experiments (Bloom et al., 1965; Orekhov et al., 1994) or more recent

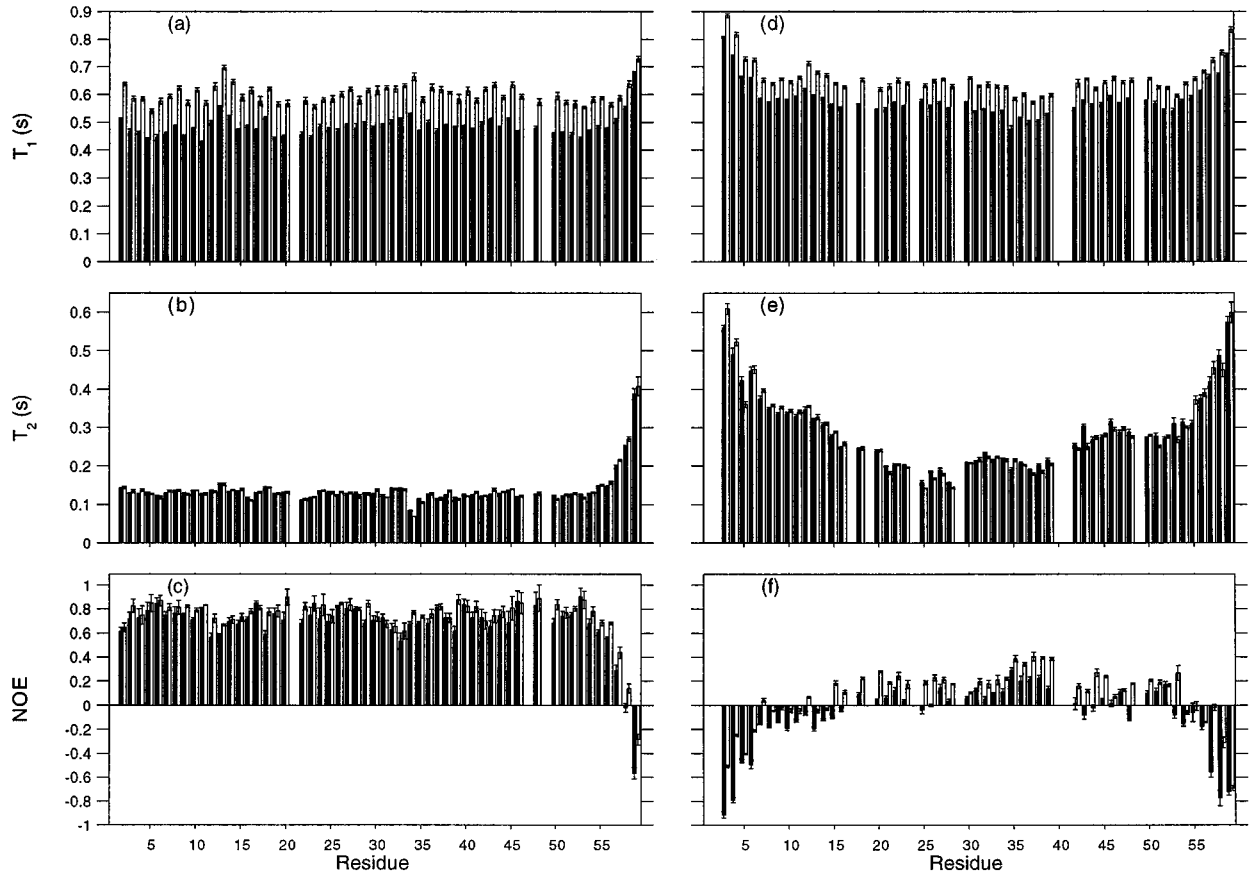

FIGURE 1: Plots of ^{15}N T_1, T_2, and steady-state $^1H-^{15}N$ NOE recorded at 14 °C. Relaxation parameters of the F_S state of the drkN SH3 domain are shown in a−c; parameters of the U_{Gdn} state are shown in d−f. Values of T_1 are shown in panels a and d, values of T_2 in b and e, and values of the steady-state NOE in panels in c and f. Shaded and open bars indicate the values of the relaxation parameters determined from data collected at 500 and 600 MHz, respectively.

off-resonance $T_{1\rho}$ experiments developed by Akke and Palmer (1996) may prove to be more useful in providing estimates of R_{ex}.

Figure 2 shows the average values of J(0 MHz) determined from data collected at both 500 and 600 MHz using eqs 1−3. In view of the above discussion, particularly in relation to the precision with which values of J(0 MHz) may be determined when an R_{ex} contribution is assumed, we have opted to report these values assuming no contribution to transverse relaxation from millisecond−microsecond time scale motions. However, for a small number of residues measured T_2 values were significantly smaller than values obtained for neighboring amino acids. In these cases R_{ex} values were calculated. For example, the T_2 value of Ser-34, in the folded state at 14 °C, showed a marked decrease with field strength; the value of T_2 measured at 600 MHz was a factor of 0.84 lower than that at 500 MHz. This decrease corresponds to an R_{ex} contribution of 4.78 s^{-1} ($\pm$0.91 s^{-1}), a factor of 4 larger than the R_{ex} values found for all other residues in the protein. Note that the cross peak for Ser-34 is well resolved and the T_2 decay curves are closely exponential. However, the T_2 values for this residue at both 500 and 600 MHz are very much lower than those of the neighboring residues suggesting the presence of additional relaxation mechanisms. Correction of the value of J(0 MHz) by the calculated R_{ex} term results in a value close to that of the neighboring residues, suggesting that such a correction is appropriate.

The values of J(0 MHz) for Leu-25 and Leu-28 in the unfolded state are noticeably larger than those adjacent to them (see Figure 2d). These differences are observed at both 14 and 30 °C, but are considerably reduced at the higher temperature. We note that when R_{ex} terms of 1.03 and 0.80 s^{-1} are included for Leu-25 and Leu-28, respectively, the values of J(0 MHz) that are obtained at 14 °C are close to those of adjacent residues.

Figure 3 illustrates the differences that arise in the measured values of the spectral density as a function of temperature. The figure shows the values of J(0 MHz) and J(516 MHz) of both the folded and unfolded states of the protein at 14 and 30 °C. The values of the spectral density function evaluated at 0 MHz are reduced at the higher temperature in both the folded and unfolded states of the domain while the overall profile of J(0 MHz) values across the molecule is unchanged. For both the folded and unfolded states of the domain the increase in sample temperature results in elevated levels of J(516 MHz); the average J(516 MHz) values increase by factors of 1.7 and 1.2 for the folded and unfolded states, respectively. Some small differences were observed in the sequential variation of J(516 MHz) at the two temperatures in both the folded and unfolded states of the domain. However, trends in the values of J(516 MHz) averaged over several residues appear to be largely unaffected by the temperature difference.

Model-Free Analysis. As discussed previously an alternative to the spectral mapping procedure employed above is to fit the measured relaxation data using the model-free spectral density function given in eq 7. Data from both the folded and unfolded states of the drkN SH3 domain were analyzed in this manner. However, because the model-free formalism characterizes the overall tumbling of a molecule

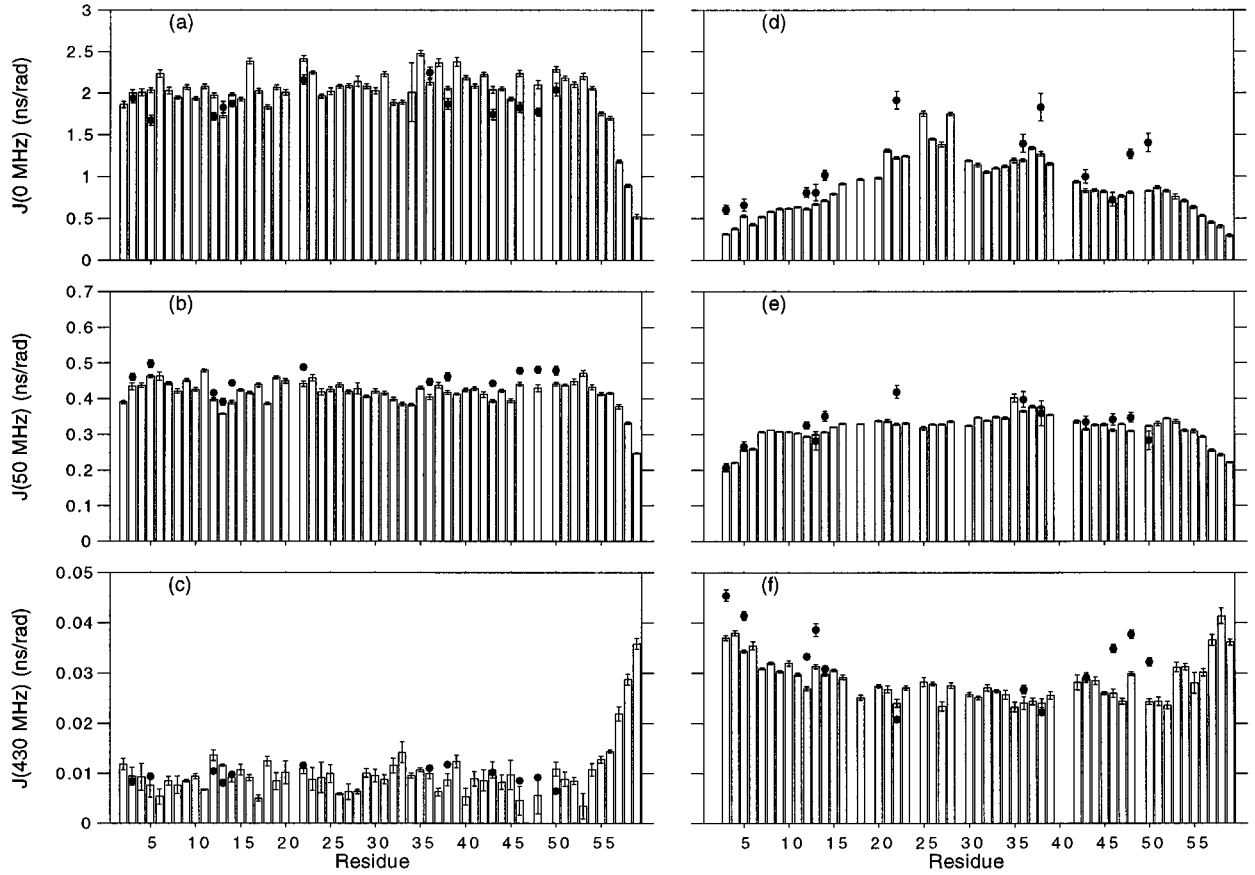

FIGURE 2: Spectral density values for the F_S a−c and the U_{Gdn} d−f states of the drkN SH3 domain (14 °C). Values of J(0 MHz) are shown in a and d, values of J(50 MHz) in b and e, and of J(430 MHz) in c and f. The solid circles indicate values of the spectral density function derived previously (Farrow et al., 1995a) from analysis of the relaxation parameters of the F_{exch} and U_{exch} states, (14 °C).

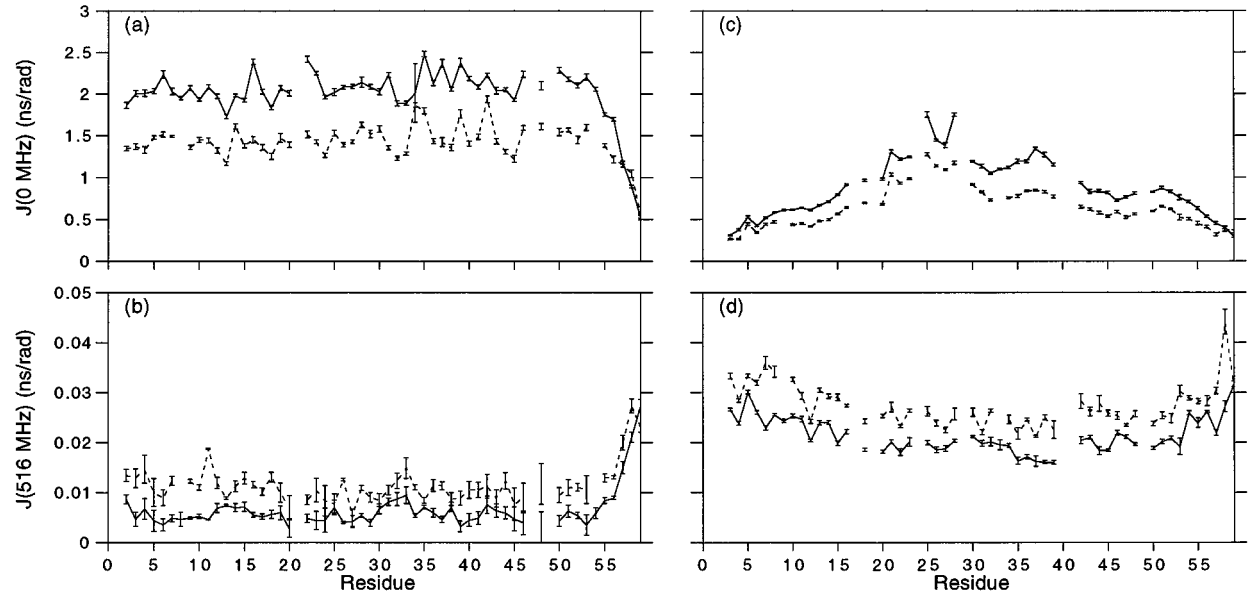

FIGURE 3: Effect of increasing temperature on the calculated values of J(0 MHz) and J(516 MHz) for residues in the F_S and U_{Gdn} states of the drkN SH3 domain. Solid and dashed lines indicate data collected at 14 and 30 °C, respectively. Data from the F_S state of the protein are shown in a and b. Data from the U_{Gdn} state of the protein are shown in c and d. Values of J(0 MHz) are shown in a and c, and values of J(516 MHz) are shown in b and d.

in terms of a single correlation time, this approach is unlikely to correctly describe the motion of an unfolded protein. As a result a cautious approach should be adopted when drawing conclusions from model-free parameters extracted from the relaxation data of the unfolded state. Values of the overall correlation time of the protein were determined by simultaneously fitting the relaxation data collected at two field strengths using the model-free spectral density function given in eq 7, and are given in Table 1. The values of the correlation time reported as "global" optima represent the value of τ_m that best fitted the relaxation data when all residues with a T_1/T_2 ratio within 1 standard deviation of the mean T_1/T_2 value were considered simultaneously. As expected the correlation times of both the folded and unfolded states of the protein were found to be shorter at higher temperatures, presumably reflecting a reduction in

Table 1: Overall Correlation Times, τ_m, Determined from Model-Free Spectral Density Function Analysis of Relaxation Data Collected at both 500 and 600 MHz[a]

	global optimum	upper quartile	lower quartile	interquartile range
folded 14 °C	6.2	6.4	6.0	0.4
folded 30 °C	4.2	4.5	4.0	0.5
unfolded 14 °C	4.1	4.7	3.3	1.4
unfolded 30 °C	3.4	3.7	2.7	1.0

[a] Values of the global optimum overall correlation time, τ_m (ns), determined for residues with T_1/T_2 ratios within 1 standard deviation of the mean ratio. Upper and lower quartile values are from the distribution of optimum τ_m values for each residue individually. Optimizations were performed using a grid search in τ_m with a step size of 0.1 ns.

solvent viscosity as a function of increased temperature (see below).

The distributions of individual τ_m optima are quite different for the folded and unfolded states of drkN SH3. We have therefore chosen to characterize these distributions in terms of the upper and lower quartile values (Sokal & Rohlf, 1981) of the individual τ_m optima (see Table 1) rather than the more familiar standard deviation of the distribution of τ_m values. In the folded state the individual τ_m values are, for the majority of residues, rather tightly distributed around the global optimum value. In the unfolded protein a wider range of values is observed, reflecting the form of the T_2 distribution shown in Figure 1e. The interquartile range (see Table 1) clearly shows the differences in the range of τ_m values in the folded and unfolded states.

Values of the order parameter squared, S^2, and the internal correlation time, τ_e, extracted from simultaneously fitting relaxation data from both field strengths are shown in Figure 4 for residues with a T_1/T_2 ratio less than 1 standard deviation from the mean value. The average values of the model-free parameters are given in Table 2 for all residues with individual τ_m optima between the upper and lower quartile values. The mean values of S^2 and τ_e for the F_S folded state of the molecule are similar to those reported in many other studies of folded proteins, and the values at 14 °C are very close to those obtained for the F_{exch} state of the drkN SH3 domain in the exchanging folded-unfolded sample, also studied at 14 °C (Farrow et al., 1995a). The order parameters of the U_{Gdn} unfolded state of the protein are considerably smaller than those of the folded protein, reflecting the increased motional freedom of this state. The average value of the order parameters determined for the U_{Gdn} unfolded state at 14 °C is also in close agreement with that obtained previously for the U_{exch} state, while the values of τ_e are shorter in the U_{Gdn} unfolded sample.

DISCUSSION

Backbone Dynamics of the F_S Folded State. The values of the spectral density function of backbone amide bond vectors were determined at a number of frequencies, (0, ω_N, and $0.86\omega_H$). At each of the frequencies examined it was found that, for the folded state of the drkN SH3 domain, the values of the spectral density function were essentially constant throughout the majority of the protein. Structural studies of the folded drkN SH3 domain have determined that the tertiary fold of the protein is extremely similar to that previously described for the homologous mammalian protein, Grb2 (Wittekind et al., 1994; Goudreau et al., 1994; Teresawa et al., 1994). The domain is composed of a β-barrel structure with no extended loops and, with the exception of the residues close to the C-terminus of the molecule, no poorly defined regions (Zhang & Forman-Kay, 1995). The compact nature of the SH3 structure suggests that it would be unlikely that different regions of the protein would exhibit large variations in dynamic behavior. The observed lack of heterogeneity in the backbone dynamics across the protein shows that this is indeed the case.

Despite the relative uniformity of backbone dynamics throughout the majority of the protein, residues C-terminal to Met-55, have spectral density function values that differ from the rest of the molecule. The decreased values of $J(0$ MHz) for these residues, and the correspondingly increased values of $J(\omega)$ evaluated at high frequencies, suggest that this portion of the protein is likely disordered in solution. This conclusion is supported by the fact that no intermediate or long-range NOEs were detected for residues C-terminal to Lys-56 within the F_S state (Zhang & Forman-Kay, 1995).

A previous study of the drkN SH3 domain in aqueous buffer, where the folded and unfolded states of the domain are in slow exchange, also concluded that there was relatively little heterogeneity in the levels of dynamics of the folded state (Farrow et al., 1995a). In the study of the F_{exch} folded state, spectral overlap restricted the number of residues (to 12) for which the backbone dynamics could be determined. In the case of the F_S state studied at high salt concentration it has been possible to monitor the dynamics of almost all of the residues in the protein. From this more extensive study it is apparent that there is little correlation between the values of the spectral density function measured throughout the protein and the location of the secondary structural elements within the molecule.

The spectral density values previously determined for the F_{exch} folded state of the drkN SH3 domain are indicated by the solid circles in Figures 2a−c. Comparison of the data from the two studies establishes that the values of the spectral density function corresponding to the F_{exch} and F_S states of drkN SH3 are only slightly different from one another, at each of the frequencies examined. The $J(0$ MHz) values of the F_S state are slightly higher, by a factor of 1.06 on average, than those of the F_{exch} state. This observation correlates well with differences in the measured viscosities of the solvents in the two studies. The solvent viscosity in the present case is a factor of 1.11 times higher than the solvent viscosity used in the study of the F_{exch} state of the protein (see Table 3). An overall correlation time, τ_m, of 5.5 ns was obtained for the F_{exch} folded state of the drkN SH3 domain on the basis of a model-free analysis of the relaxation data (Farrow et al., 1995a). The correlation time resulting from a model-free analysis of the F_S folded state of the domain gives an overall correlation time of 6.2 ns, an increase in keeping with the differences in the viscosities of the solvents in the two studies.

Comparative structural studies of the F_S and F_{exch} folded states of the drkN SH3 domain suggest that the structure of the two states are very similar on the basis of similarities in $^3J_{NH\alpha}$ coupling constants, backbone chemical shifts and NOE connectivities (Zhang & Forman-Kay, 1995). The observation that the magnitudes of the spectral density functions are similar in the two folded states suggests that the increased stability of the domain under high salt conditions is not correlated with reduced levels of internal dynamics at any of the frequencies examined.

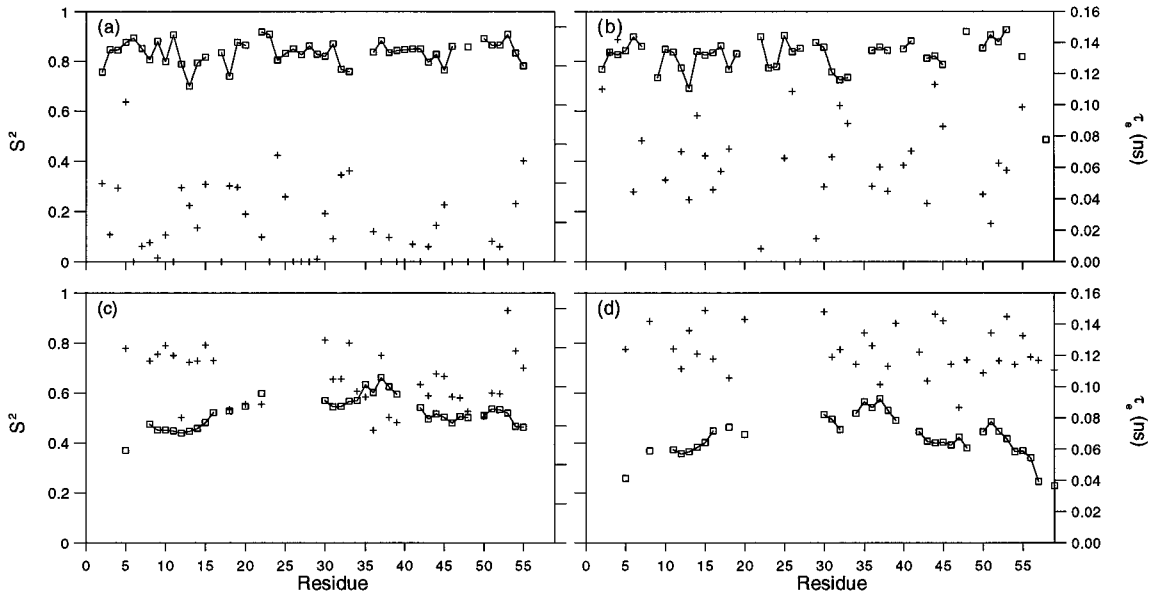

FIGURE 4: Values of the model-free parameters: S^2, the generalized order parameter squared, and τ_e, the correlation time describing internal motions of the amide bond vector. Data are shown only for residues that have a T_1/T_2 ratio less than 1 standard deviation from the mean value. Values for the F_S state of the drkN SH3 domain are shown in a and b, while data from the U_{Gdn} state are shown in c and d. Values of S^2 are indicated by the open squares joined by solid lines where data from consecutive residues were collected, while values of τ_e are indicated by crosses. Panels a and c show the values of the model-free parameters determined at 14 °C, while panels b and d illustrate the values determined at 30 °C. In panel b the τ_e values of seven residues are greater than the abscissa maximum.

Table 2: Values of Model-Free Parameters[a]

	S^2	τ_e (ns)
folded 14 °C	0.83 ± 0.05	0.021 ± 0.021
	[0.85 ± 0.05]	[0.033 ± 0.036]
folded 30 °C	0.84 ± 0.05	0.069 ± 0.047
unfolded 14 °C	0.51 ± 0.06	0.103 ± 0.018
	[0.50 ± 0.17]	[0.360 ± 0.386]
unfolded 30 °C	0.41 ± 0.10	0.126 ± 0.027

[a] Average values and standard deviations of model-free parameters determined for residues with τ_m values between the upper and lower quartile values (Sokal & Rohlf, 1981) of the distribution of individual overall correlation times. Values of the model-free parameters previously determined for the F_{exch} and U_{exch} states of the drkN SH3 domain at 14 °C (Farrow et al., 1995a) are given in square brackets.

Table 3: Values of Solvent Viscosity[a]

	14 °C	30 °C
0.05 M sodium phosphate	1.204	0.814
0.4 M sodium sulfate + 0.05 M sodium phosphate	1.332	0.916
2 M Gdn HCl + 0.05 M sodium phosphate	1.219	0.846

[a] Values of solvent viscosities (expressed in centipoise) were determined using an Ostwald viscometer and standard analytical techniques (Cantor & Schimmel, 1980).

Backbone Dynamics of the U_{Gdn} Unfolded State. A number of studies have been performed to characterize the internal dynamics of the unfolded states of proteins (Torchia et al., 1975; van Mierlo et al., 1993; Alexandrescu & Shortle, 1994; Logan et al., 1994; Redfield et al., 1994; Farrow et al., 1995a; Frank et al., 1995; Buck et al., 1996). In order to better interpret the dynamics data of the U_{Gdn} state, it is useful to briefly review the results of these other studies. In all cases the unfolded states of the molecules studied possess levels of motion throughout the protein or in certain regions of the protein which exceed those typically associated with the corresponding native states. While the extent and amplitude of the motions observed in these studies varies widely, it is generally the case that the amount of residual secondary and tertiary structure in the protein is inversely related to the level of internal dynamics.

Dobson and co-workers have studied the partially unfolded states of two proteins, a molten globule state of interleukin-4 (IL-4) at low pH (Redfield et al., 1994), and TFE-denatured lysozyme (Buck et al., 1996). Under these conditions both proteins contain significant amounts of helical structure and are stabilized by the presence of disulfide bonds but lack extensive tertiary interactions. In the case of IL-4, the order parameters of residues in the molten globule are slightly lower than those of the native protein, with regions involved in helical structure having order parameters similar to those in folded proteins ($S^2 > 0.8$). A significant decrease in order parameters relative to that of the folded state was observed in the N-terminus of one of the helices of the protein, suggestive of a local destabilization of this region of the molecule. In the study of TFE-denatured lysozyme, high order parameters were found in the centers of all the persistent native-like helices. At the termini of several of the helices, and in a region that adopts a non-native α-helical structure in the presence of TFE, lower order parameters and increased values of τ_e were observed, indicating considerable flexibility of these regions in the partially unfolded state.

While involvement in persistent secondary structure appears to be the principal factor in determining the level of mobility of the protein backbone in both IL-4 at low pH and TFE-denatured lysozyme, further analysis of the data from the latter study identified a number of other determinants which influence the dynamics of the unfolded state. Principal among these factors was the presence of disulfide bonds. It was demonstrated that residues at positions distant from the cysteines involved in the disulfide bonds were often those with the lowest order parameters. This relationship was particularly apparent in the region of the protein that contained little secondary structure. It was also shown that highly mobile portions of the protein were often linked to the presence of glycine residues. This is likely due to the absence of motional constraints because of the small amino

acid side chain (R = H) of the glycine. Finally, a correlation was observed between the hydrophobicity profile of the molecule and the variation of S^2, with hydrophobic regions possessing lower levels of backbone motion.

Another highly disordered molecule that has been studied extensively is a 131 residue fragment of staphylococcal nuclease, Δ131Δ, which possesses little residual structure even in the absence of denaturants (Alexandrescu et al., 1994; Alexandrescu & Shortle, 1994). Analysis of the NMR relaxation data from this molecule has established a region of higher order parameters in the portion of the protein that contains the majority of the residual structure. Contributions to transverse relaxation rates from slower motional processes on millisecond to microsecond time scales were also found predominantly in this portion of the molecule. The remainder of the protein is significantly more mobile with values of $S^2 < 0.5$ and correlation times, τ_e, in the range 0.4−1.2 ns. These τ_e values are considerably longer than those describing backbone motions in folded proteins. Large internal correlation times and low order parameters were also reported for TFE-denatured lysozyme (Buck et al., 1996) and a partially folded mutant of BPTI (van Mierlo et al., 1993). Finally, it was noted that the motionally restricted region of Δ131Δ corresponds to a hydrophobic region of the molecule suggesting that the hydrophobic collapse of the protein influences the backbone dynamics of the unfolded state.

The partially folded form of BPTI studied by Creighton and co-workers (van Mierlo et al., 1993) possesses a region in which many of the structural features of the native protein are present as well as an unfolded N-terminal segment with considerably higher levels of internal dynamics. The dynamics of this segment decrease from the N-terminus and approach a level typical of the core of the molecule over a span of approximately 18 residues.

NMR structural studies of a urea-denatured immunoglobulin binding domain of streptococcal protein G (GB1) suggest that this form of the molecule does not contains any ordered, native or non-native, structure (Frank et al., 1995). In contrast to the other studies discussed above the extent of sub-nanosecond time scale motions within the protein are fairly uniform (S^2 ranging between 0.4 and 0.5) across the molecule. The only exception to this occurs at the N- and C-termini where there is an increase in the mobility of the backbone leading to values of S^2 as low as 0.1. Three segments of GB1 were identified on the basis of the requirement of an exchange line-broadening term to account for locally reduced transverse relaxation rates. However, it was noted that the order parameters of these regions of the protein were not perturbed by the slower time scale motions. A study of a thermally denatured 36 residue collagen peptide by Torchia and co-workers (1975) also revealed a similar pattern of dynamics to that observed in GB1. With the exception of residues close to the termini of the molecule the correlation times of the α-carbons were observed to show little variability as a function of sequence, consistent with motions of a chain in which all residues possess similar motional properties and have significant levels of independence.

Thus, it is clear from previous studies of the backbone dynamics of the unfolded states of proteins that the levels of backbone motion are closely linked to the amount of secondary structure, residual or otherwise, in the molecule. Such structure can confer levels of dynamics similar to those seen in folded proteins. The presence of disulfide bonds and hydrophobic regions results in a restriction of backbone mobility, while glycine residues potentially confer higher levels of backbone motion. Proteins which possess very low levels of ordered structure are characterized by rather uniform levels of nanosecond time scale dynamics, often with increased levels of motion associated with only a few residues near the termini of the molecule.

The present dynamics study of the drkN SH3 domain indicates that unlike GB1 or the collagen peptide and, in contrast to the folded state of the molecule, $J(\omega)$ values for the unfolded state show a significant degree of variation. This is most notable in the plots of the value of J(0 MHz) with respect to residue, Figure 2d. The values of J(0 MHz) gradually increase from the N-terminus of the molecule toward a maximum in the vicinity of residues 25−28. The gradual decrease of J(0 MHz) values toward the minimum value at the C-terminus of the molecule is interrupted by two local maxima at Tyr-37 and Asn-51.

Values of the spectral density function evaluated at zero-frequency are directly related to the correlation time associated with the overall re-orientation of the molecule. In the case of the U_{Gdn} state of the drkN SH3 domain the observed pattern of J(0 MHz) is more similar to that seen in the unfolded portion of a mutant of BPTI (see above) than to that observed in denatured collagen. Recall that in the collagen study the correlation times estimated at each α-carbon position along the backbone were uniform, with the exception of those close to the termini of the molecule which were somewhat shorter (Torchia et al., 1975). The concerted variations in the values of the spectral density function at zero-frequency for the U_{Gdn} state of the drkN SH3 domain suggest that in this state the domain is not undergoing simple segmental motion. Rather, the extent of low frequency motion in the molecule appears to be correlated with the distance of a particular residue from the termini. Thus, motion of residues close to the termini of the protein requires cooperative movement of only small sections of the polypeptide, while re-orientation of the residues in the central region of the molecule requires motion of a much larger portion of the protein. The high values of J(0 MHz) toward the center of the drkN SH3 domain are of similar magnitude to those seen in the F_S folded state of the protein, suggesting that this portion of the molecule is relatively compact and thus tumbles more slowly in solution.

Molecular dynamics simulations indicate that the rotational correlation times of disordered linear polymers may exhibit characteristic bell-shaped profiles, similar in form to the pattern of J(0 MHz) values observed for the U_{Gdn} state of the drkN SH3 domain (Hu et al., 1990). Predictions of rotational correlation times obtained from long time scale dynamics simulations have been compared with experimental results from tryptophan fluorescence depolarization measurements performed on 17-residue synthetic polypeptides to probe variations in rotational correlation times at different positions within the molecule. Both the simulations and the accompanying experimental data show that correlation times at the center of the molecule are longer than those toward the termini. In addition to the underlying bell-shaped profile of rotational correlation times determined from the molecular dynamics simulation, it was demonstrated that the amino acid sequence influences the mobility of the peptide, giving rise to local maxima and minima in the correlation time profile. When long time scale molecular dynamics studies were performed on two proteins, the adrenocorticotropic hormone

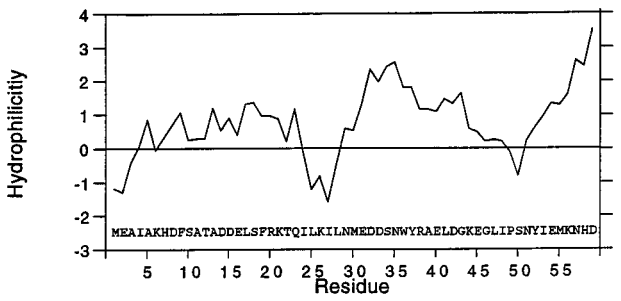

FIGURE 5: Kyte−Doolittle hydrophilicity plot for the drkN SH3 domain generated using an averaging window of size 7 (Wisconsin Package GCG Version 8.1).

(ACTH) and glucagon, the mobility profile was observed to cluster in discrete protein domains, indicative of the influence of the protein primary sequence (Hu et al., 1990). Thus, it may be that local maxima and minima in the *J*(0 MHz) spectral density profile of the unfolded SH3 domain are due to specific primary-sequence-related interactions which influence the local flexibility of the molecule.

A correlation has been established between the hydrophilicity of residues of proteins in unfolded states and the levels of backbone dynamics (Alexandrescu & Shortle, 1994; Buck et al., 1996). It was demonstrated that residues with low order parameters occur in hydrophilic regions of the protein, while residues in hydrophobic regions of the molecule have larger order parameters, indicative of more restricted motion. The observed correlation between the hydration propensity of a residue and restriction of its motion is not surprising. Residues with high hydrophilicity indices are more likely to exist in flexible solvent-exposed conformations, whereas hydrophobic residues are likely to be sequestered in restricted conformations within the compact portions of the molecule. Figure 5 shows a plot of hydrophilicity as a function of sequence for the drkN SH3 domain. The plot was generated using a Kyte−Doolittle hydrophilicity algorithm, and the values shown represent an average over a window of seven residues (Wisconsin Package, GCG, Version 8.0.1). Comparison of Figure 5 and Figure 2d shows that the residues with the largest values of *J*(0 MHz) in the unfolded state, Leu-25 to Leu-28, correspond to a local minimum in the hydrophilicity plot. Such a correlation suggests that limited hydrophobic collapse may influence the extent of zero-frequency motion in the U_{Gdn} state of the drkN SH3 domain. Additionally, it is interesting to note that local minima in the hydrophilicity plot at residues 40 and 50 correspond closely to local maxima in the *J*(0 MHz) profile of the unfolded state.

Chaotropic agents such as urea and guanidinium chloride act to unfold proteins by disrupting non-covalent interactions within native protein structures (Matthews, 1993). It has been shown that guanidinium chloride interacts directly with the unfolded protein via multiple hydrogen bonds (Makhatadze & Privalov, 1992). This mechanism serves to immobilize the denaturant on the polypeptide surface. The assertion that the denaturant interacts directly with the unfolded peptide is supported by the observation that the amide proton exchange rates of the unfolded state are considerably lower in the presence of guanidinium chloride than they are in aqueous buffer (Zhang & Forman-Kay, 1995). Interactions between the denaturant and the peptide could potentially lead to the fixation of different protein groups with respect to one another, thereby decreasing the flexibility of the denatured molecule. In the drkN SH3 domain the locations of the polar residues that are likely to form hydrogen bonds with the denaturant molecule do not correlate well with the observed maxima in the *J*(0 MHz) spectral density profile, since such residues are distributed fairly uniformly across the protein. Moreover the *J*(0 MHz) profiles for the U_{exch} and U_{Gdn} states of drkN SH3 are similar. It is therefore unlikely that the denaturant rigidifies the U_{Gdn} state of the molecule.

In the unfolded protein, variations in the values of the spectral density at 50 and 430 MHz as a function of position in primary sequence are much less pronounced than those observed at 0 MHz (Figures 2d−f). At the higher frequencies the levels of motion are roughly constant between Asp-8 and Ser-50. Relative to the rest of the protein, residues at the N- and C-termini have reduced *J*(50 MHz) and increased *J*(430 MHz) values. Increased levels of disorder (usually characterized by low values of S^2) for the termini have been observed in many studies of folded proteins and have also been reported in studies of the backbone dynamics of unfolded proteins (Torchia et al., 1975; van Mierlo et al., 1993; Logan et al., 1994; Redfield et al., 1994; Frank et al., 1995; Buck et al., 1996). In the case of folded proteins the observation of increased disorder at the termini of the molecule is often attributed to the fact these portions of the protein are "unstructured" in solution. The fact that similar patterns of dynamics are observed in many "unfolded" proteins and, in the present case, at the termini of the unfolded drkN SH3 domain suggests the presence of different levels of motional constraints within unfolded states of proteins with more restricted motions in the central portion of such molecules relative to regions close to the termini.

Values of the spectral density function that were previously determined for the U_{exch} state of the drkN SH3 domain (Farrow et al., 1995a) are indicated by solid circles in Figure 2d−f. The plot of *J*(0 MHz) as a function of sequence in the unfolded protein (Figure 2d) shows that, while the trends in the values of the spectral density function across the protein are similar in the two studies, the values determined in the presence of denaturant are significantly lower than those obtained for the sample in aqueous buffer near neutral pH. In contrast, at the higher frequencies studied, 50 and 430 MHz, the average values of the spectral density function for U_{exch} and U_{Gdn} states of the domain are not significantly different. In the case of the F_S and F_{exch} folded states of the drkN SH3 domain (see above), differences in the magnitudes of *J*(0 MHz) could be explained on the basis of the different solvent viscosities in the two studies. A similar analysis fails to explain the differences in *J*(0 MHz) values observed for the two unfolded states of the protein. In this case the viscosities of the two solvents are similar (see Table 3) whereas the mean value of *J*(0 MHz) in the U_{Gdn} state is a factor of 0.78 lower than in the U_{exch} state. However, the lack of correlation between solvent viscosity and the observed values of *J*(0 MHz) is not unexpected. The overall correlation time of a protein, and thus the spectral density function at zero-frequency, is influenced by many factors including the shape of the molecule, the microscopic viscosity at the surface of the protein, and the extent of persistent structure. For roughly spherical proteins, Stoke's law may be used to estimate the effective hydrodynamic radius of a molecule from information about the overall correlation time and the bulk solvent viscosity. In the absence of detailed structural data and hydrodynamic calculations, interpretation of the observed differences in the magnitude of the spectral density

functions at zero-frequency in the two studies must be qualitative (see below).

Residual structure in the U_{Gdn} and U_{exch} forms of the drkN SH3 domain has been characterized extensively (Zhang & Forman-Kay, 1995, 1996) and this information provides a necessary and valuable framework both for the interpretation of the results of the current study and for comparison of the dynamics of the drkN SH3 domain with previous studies of the internal dynamics of unfolded proteins. Comparative structural studies of U_{Gdn} and U_{exch} states have shown that the amount of structure in the U_{exch} unfolded state exceeds that observed in the presence of guanidinium chloride. The existence of different levels of structure in the central portion of the U_{Gdn} and U_{exch} states of the protein is supported by the observation that the residues in this region show the greatest $C^{\alpha}H$, NH and ^{15}N chemical shift differences between the two unfolded states (Zhang & Forman-Kay, 1995). Additional support for the contention that the U_{exch} state of the protein is more compact than the U_{Gdn} state is provided by the observation that fewer medium-range amide−amide NOEs are observed in the guanidinium chloride-denatured state (Zhang & Forman-Kay, 1996). Moreover, it has been found that reducing the temperature of the exchanging folded−unfolded sample to 5 °C leads to extreme broadening of the resonances of residues 23−28 of the U_{exch} state (Zhang & Forman-Kay, 1996). In contrast, reduction of the temperature of the unfolded sample in the presence of guanidinium chloride does not result in excessive line broadening of these resonances. There does, however, appear to be some evidence for slow motional processes in this region of the U_{Gdn} state of the drkN SH3 domain (Figure 2d). As described above, T_2 measurements at two field strengths indicate an exchange contribution to the transverse relaxation of residues Leu-25 and Leu-28.

The different behavior of residues 23−28 of the U_{Gdn} and U_{exch} states of drkN SH3 as the temperature of the sample is reduced correlates well with the observed differences in the amount of structure in these two states. The extreme line-broadening that is observed at lower temperatures in the U_{exch} state of drkN SH3 likely reflects the preferential stabilization of certain conformational microstates, which results in a reduction in the rate of exchange between these states. The fact that micro-states of the U_{exch} state of drkN SH3 are more readily stabilized than those of the U_{Gdn} form of the molecule suggests that the U_{exch} state may be inherently more structured at the temperatures used in the current study. The additional structure present in the U_{exch} unfolded state of the domain results in slower molecular tumbling in solution, giving rise to the higher values of $J(0)$ relative to the U_{Gdn} state.

Effect of Temperature on Backbone Dynamics. The measurement of relaxation parameters and the subsequent determination of values of the spectral density function at two temperatures permits examination of the extent to which the backbone dynamics of the folded and unfolded states of the protein are affected by an increase in temperature. The most significant changes in the spectral density function of both the folded and unfolded states of the protein with temperature relate to differences in the overall correlation time of the molecule. For both states of the protein, the average value of $J(0)$ at 30 °C is a factor of 0.7 smaller than that determined at 14 °C. Measurements of solvent viscosity at the two temperatures (Table 3) reveals that, for both the 0.4 M Na_2SO_4 and 2 M guanidinium chloride solutions, an increase in temperature from 14 to 30 °C is accompanied by a reduction in viscosity by a factor of 0.7. The corresponding observed reduction in $J(0)$ can thus be explained by changes in solvent viscosity, resulting from differences in temperature (Cantor & Schimmel, 1980). This result is particularly interesting in the case of the unfolded protein: it suggests that the U_{Gdn} unfolded state of the molecule responds to changes in viscosity in the same manner as the F_S folded state. The fact that the changes in $J(0)$ of the denatured protein correlate well with temperature-induced changes in viscosity suggests that the differences in $J(0)$ observed between the U_{Gdn} and U_{exch} unfolded states of the protein at a single temperature and at similar solvent viscosity are the result of different levels of residual structure in the two states (see above).

The average values of the spectral density function determined at 516 MHz for the folded and unfolded states of the drkN SH3 domain increase by factors of 1.7 and 1.2, respectively, when the sample temperature is raised from 14 to 30 °C. Interpretation of these changes in terms of an increase in internal high-frequency motions in the protein is complicated by the fact that the overall molecular tumbling rate influences the measured values of the spectral density function at high frequencies. Therefore, in order to examine the temperature dependence of high-frequency motions, it is necessary to consider contributions arising from the temperature dependence of the overall correlation time. To assess the magnitudes of these contributions we consider the form of the spectral density function described by Lipari and Szabo (1982a,b). Simulations using parameters typical of those for a folded protein ($S^2 = 0.8$; $\tau_e = 20$ ps) and assuming a value of τ_m close to that observed for the drkN SH3 domain (5 ns), indicate that the first term on the right hand side of eq 7 [i.e., $S^2\tau_m/(1 + (\omega\tau_m)^2)$] dominates the value of the spectral density function at 500 MHz, contributing ∼89% of $J(500\text{ MHz})$. In contrast, calculations with model-free parameters similar to those associated with unfolded proteins ($S^2 = 0.5$; $\tau_e = 100$ ps) and setting τ_m to 5 ns establish that the second term in eq 7 [i.e., $(1 - S^2)\tau/(1 + (\omega\tau)^2)$] contributes 82% of the value of the spectral density function at 500 MHz. The implications of these results for the folded state of the protein are that, for molecules of the size considered in this study where $\omega_H\tau_m \gg 1$, the high-frequency components of the spectral density function scale as the inverse of the overall correlation time of the protein. Thus, the observed increase in $J(516\text{ MHz})$ that accompanies an increase in temperature is primarily due to a reduction in the overall correlation time of the protein. As noted above, the viscosity of the 0.4 M Na_2SO_4 buffer falls by a factor of 0.7 upon increasing the temperature from 14 to 30 °C. Assuming Stoke's law this reduction in viscosity will be accompanied by a reduction in the overall correlation time of the protein also by a factor of 0.7. On the basis of the foregoing arguments the contribution from the overall tumbling of the molecule to the spectral density function at ∼500 MHz will increase by a factor of roughly 1.4. Thus, the factor of 1.7 increase in the value of $J(516\text{ MHz})$, observed when the temperature of the sample is increased, arises primarily from the reduction in the overall correlation time of the molecule. For the unfolded state, the contribution to the spectral density function at high frequency from the overall correlation time is much less significant. Therefore the observed increase in $J(516\text{ MHz})$ upon increasing the

temperature of the U_{Gdn} sample likely reflects increased levels of high-frequency motions.

In order to further investigate the relationship between temperature and the level of backbone dynamics we have analyzed the experimental data using a model-free approach. Note that a cautious approach should be adopted when interpreting model-free parameters of unfolded protein states, and we have chosen only to compare the results in a qualitative fashion. From Table 2 and Figure 4 it is seen that the values of S^2 for the folded protein at the two temperatures remain roughly constant, and while there is an increase in the value of the correlation time of internal motions, τ_e, the uncertainties associated with these data are large. For the unfolded state of the protein the average value of S^2 falls from 0.51 to 0.41 upon increasing the temperature from 14 to 30 °C, while the average value of τ_e remains roughly constant.

Together, the spectral density mapping studies and model-free analyses of the relaxation data suggest that the folded and the unfolded states of the molecule respond quite differently to changes in temperature. Increasing the temperature of the unfolded state clearly leads to more extensive high-frequency motion as reflected by increased values of J(516 MHz) and lower values of S^2. These changes are not seen when the temperature of the folded state is increased. A likely explanation of the difference in behavior relates to the fact that the structure of the folded state is stabilized by many interactions. As the temperature of the folded sample is increased some of the interactions will likely be lost; however, those remaining will suffice to maintain the folded structure of the protein and therefore limit the dynamics. This cooperative stabilization is not present in the unfolded state and therefore increased temperatures simply result in higher levels of motion within the protein.

CONCLUSIONS

A previous study of the backbone dynamics of a mixture of F_{exch} folded and U_{exch} unfolded states of the drkN SH3 domain was hampered by significant overlap in the NMR spectra, which limited the number of residues available for analysis. In this paper we have studied the fully folded (F_S) and unfolded (U_{Gdn}) states of the protein that are stabilized by modification of solvent conditions. The reduced spectral overlap under these conditions permits a more extensive characterization and comparison of the dynamics of the folded and unfolded states than was previously possible.

The F_S folded state of the protein, obtained in the presence of 0.4 M Na_2SO_4, shows little variation in the levels of internal dynamics across the molecule. The absolute values of the spectral density function of the F_S state of the drkN SH3 domain are close to those previously determined for the F_{exch} state. One of the issues that was addressed in the current study was the determination of the extent to which the internal dynamics of a folded protein influence its stability. In the case of the drkN SH3 domain, the similarity in the spectral density values of the F_S and F_{exch} states suggests that the increased stability of the molecule in the presence of 0.4 M Na_2SO_4 does not result from a reduction in the level of picosecond−nanosecond time scale internal dynamics in the protein. Rather, it appears that the increased salt concentration stabilizes the protein, likely due to electrostatic shielding of a cluster of acidic residues.

The extensive characterization of the backbone dynamics of the unfolded state of the drkN SH3 domain, possible when the protein is studied in 2 M guanidinium chloride, reveals a striking pattern in the variation of J(0 MHz) across the protein. The bell-shaped form of the profile suggests that the motional properties of the unfolded molecule are not those of a disordered linear chain undergoing random segmental motion. Rather, the shape of the profile and the magnitude of the J(0 MHz) values in the center of the sequence indicate that the protein adopts a compact conformation in which residues reorient in a concerted manner. The observation that the maximum in the J(0 MHz) profile is associated with a region of hydrophobic residues suggests that the compaction of the central portion of the unfolded domain may be the result of hydrophobic collapse. Additionally, the observed local variations (over 5−10 residues) in the J(0 MHz) profile is consistent with the influence of local interactions, directly related to the primary sequence of that portion of the molecule, on the mobility of the unfolded protein.

The measured values of the spectral density function evaluated at zero-frequency suggest a higher degree of compaction for the U_{exch} unfolded state relative to the U_{Gdn} unfolded state produced by addition of guanidinium chloride. The extreme exchange broadening observed in spectra of the U_{exch} state at lower temperatures, but not seen in the U_{Gdn} state of the protein, and the higher number of medium-range amide−amide NOEs in the U_{exch} state are consistent with this interpretation. While these data indicate that the U_{Gdn} state of the domain is more "unfolded" than the U_{exch} state, the available data also indicate that the motion of the U_{Gdn} state of the protein is not completely unconstrained and that some level of compaction exists within the molecule.

Changes in temperature have been shown to produce different effects in the internal dynamics of the folded and unfolded states of the domain. The level of disorder, as reported by S^2, of the backbone of the folded protein is not significantly affected by an increase in the temperature from 14 to 30 °C. In contrast, a similar change in temperature results in an increase in the backbone mobility of the unfolded state of the protein, reflecting the lack of cooperative interactions in this form of the molecule.

Previous studies of the backbone dynamics of unfolded or partly unfolded proteins indicate that the levels of motion are linked to the amount of residual structure. In the case of the U_{Gdn} state of the drkN SH3 domain, structural studies reveal little evidence for either secondary or tertiary structure; however, it is clear from the values of J(0 MHz) determined for residues in the center of the unfolded molecule that there is a significant degree of compaction within the unfolded state. The J(0 MHz) spectral density profile of the U_{Gdn} state of the drkN SH3 domain suggests that the degree of this compaction falls toward the termini of the molecule. The profiles of higher frequency motions within the unfolded protein indicate that these motions are not influenced by the overall collapse of the molecule. Together the spectral density profiles at both high and low frequencies, and the available structural information (Zhang & Forman-Kay, 1995, 1996) suggest a molecule which becomes progressively more condensed from the termini of the protein to the center, composed throughout of transient turn-like structures, with residues proximal to the termini of the molecule exhibiting increased levels of high-frequency motions.

ACKNOWLEDGMENT

We thank Dr. Tony Pawson for providing the plasmid used in the expression of the SH3 domain and Drs. Dennis Torchia and Atilla Szabo, NIH, Bethesda, MD, and Dr. Benoit Roux, Université de Montréal, for valuable discussions.

SUPPORTING INFORMATION AVAILABLE

One figure showing examples of the 2D correlation spectra used to extract the ^{15}N relaxation parameters, and 10 tables containing the T_1, T_2, and NOE values for the F_S and U_{Gdn} states of the drkN SH3 domain determined at 500 and 600 MHz and at 14 and 30 °C; the values of the spectral density function of the F_S and U_{Gdn} states at 14 and 30 °C; and the values of the model-free spectral density parameters determined for the F_S and U_{Gdn} states at 14 and 30 °C (12 pages). See any current masthead page for ordering information.

REFERENCES

Abragam, A. (1961) *Principles of Nuclear Magnetism*, Clarendon Press, Oxford.

Akke, M., & Palmer, A. G., III (1996) *J. Am. Chem. Soc. 118*, 911−912.

Akke, M., Skelton, N. J., Kördel, Palmer, A. G., III, & Chazin, W. J. (1993) *Biochemistry 32*, 9832−9844.

Alexandrescu, A. T., & Shortle, D. (1994) *J. Mol. Biol. 242*, 527−546.

Alexandrescu, A. T., Abeygunawardana, C., & Shortle, D. (1994) *Biochemistry 33*, 1063−1077.

Arcus, V. L., Vuilleumier, S., Freund, S. M. V., Bycroft, M., & Ferst, A. (1995) *Proc. Nat. Acad. Sci. U.S.A 91*, 9412−9416.

Bloom, M., Reeves, L. W., & Wells, E. J. (1965) *J. Chem. Phys. 42*, 1615−1624.

Buck, M., Schwalbe, H., & Dobson, C. M. (1995) *Biochemistry 34*, 13219−13232.

Buck, M., Schwalbe, H., & Dobson, C. M. (1996) *J. Mol. Biol. 257*, 669−683.

Cantor, C. R., & Schimmel, P. R. (1980) *Biophysical Chemistry*, Freeman, San Francisco, CA.

Carrington, A., & McLachlan, A. D. (1967) *Introduction to Magnetic Resonance*, Harper, New York.

Clore, G. M., Szabo, A., Bax, A., Kay, L. E., Driscoll, P. C., & Gronenborn, A. M. (1990) *J. Am. Chem. Soc. 112*, 4989−4991.

Delaglio, F., Grzesiek, S., Vuister, G. W., Zhu, G., Pfeifer, J., & Bax, A. (1995) *J. Biomol. NMR 6*, 277−293.

Dobson, C. M. (1992) *Curr. Opin. Struct. Biol. 2*, 6−12.

Farrow, N. A., Muhandiram, R., Singer, A. U., Pascal, S. M., Kay, C. M., Gish, G., Shoelson, S. E., Pawson, T., Forman-Kay, J. D., & Kay, L. E. (1994) *Biochemistry 33*, 5984−6003.

Farrow, N. A., Zhang, O., Forman-Kay, J. D., & Kay, L. E. (1995a) *Biochemistry 34*, 868−878.

Farrow, N. A., Zhang, O., Szabo, A., Torchia, D. A., & Kay, L. E. (1995b) *J. Biomol NMR 6*, 153−162.

Feng, Y., Sligar, S. G., & Wand, J. A. (1994) *Nat. Struct. Biol. 1*, 30−35.

Frank, M. K., Clore, G. M., & Gronenborn, A. M. (1995) *Protein Sci. 4*, 2605−2615.

Goudreau, N., Cornille, F., Duchesne, M., Parker, F., Tocqué, B., Garbay, C., & Roques, B. P. (1994) *Nat. Struct. Biol. 1*, 898−907.

Grzesiek, S., & Bax, A. (1993) *J. Am. Chem. Soc. 115*, 12593−12594.

Hu, Y., MacInnis, J. M., Cheryil, B. J., Fleming, G. R., Freed, K. F., & Perico, A. (1990) *J. Chem. Phys. 93*, 822−836.

Kamath, U., & Shriver, J. W. (1989) *J. Biol. Chem. 264*, 5586−5592.

Kay, L. E., Torchia, D. A., & Bax, A. (1989) *Biochemistry 28*, 8972−8979.

Kördel, J., Skelton, N. J., Akke, M., Palmer, A. G., III, & Chazin, W. J. (1992) *Biochemistry 31*, 4856−4866.

Lim, W. A., Fox, R. O., & Richards, F. M. (1994) *Protein Sci. 3*, 1261−1266.

Lipari, G., & Szabo, A. (1982a) *J. Am. Chem. Soc. 104*, 4546−4559.

Lipari, G., & Szabo, A. (1982b) *J. Am. Chem. Soc. 104*, 4559−4570.

Logan, T. M., Thériault, Y., & Fesik, S. W. (1994) *J. Mol. Biol. 236*, 637−648.

Maignan, S., Guilloteau, J.-P., Fromage, N., Arnoux, B., Becquart, J., & Ducruix, A. (1995) *Science 268*, 291−293.

Makhatadze, G. I., & Privalov, P. L. (1992) *J. Mol. Biol. 226*, 491−505.

Mandel, A. M., Akke, M., & Palmer, A. G., III (1995) *J. Mol. Biol. 246*, 144−163.

Markley, J. L., Horsley, W. J., & Klein, M. P. (1971) *J. Chem. Phys. 55*, 3604−3605.

Matthews, R. C. (1993) *Annu. Rev. Biochem 62*, 653−83.

Neri, D., Billeter, M., Wider, G., & Wüthrich, K. (1992) *Science 257*, 1559−1563.

Orekhov, V. Yu., Pervushin, K. V., & Arseniev, A. S. (1994) *Eur. J. Biochem. 219*, 887−896.

Palmer, A. G., III (1993) *Curr. Opin. Biotechnol. 4*, 385−391.

Palmer, A. G., III, Rance, M., & Wright, P. E. (1991) *J. Am. Chem. Soc. 113*, 4371−4380.

Pawson, T. (1995) *Nature 373*, 573−580.

Press, W. H., Flannery, B. P., Teukolsky, S. A., & Vetterling, W. T. (1986) *Numerical Recipes*, Cambridge University Press, Cambridge.

Redfield, C., Smith, R. A. G., & Dobson, C. M. (1994) *Nat. Stuct. Biol. 1*, 23−29.

Schlessinger, J. (1993) *Trends. Biochem. Sci. 18*, 273−275.

Shortle, D. (1993) *Curr. Opin. Struct. Biol. 3*, 66−74.

Sokal, R. R., & Rohlf, F. J. (1981) *Biometry*, W. H. Freeman and Company, New York.

Stone, M. J., Chandrasekhar, K., Holmgren, A., Wright, P. E., & Dyson, H. J. (1993) *Biochemistry 32*, 426−435.

Teresawa, H., Kohda, D., Hatanaka, H., Tsuchiya, S., Ogura, K., Ishii, S., Mandiyan, V., Ullrich, A., Schlessinger, J., & Inagaki, F. (1994) *Nat. Struct. Biol. 1*, 891−897.

Torchia, D. A., Lyerla, J. R., Jr., & Quattrone, A. J. (1975) *Biochemistry 14*, 887−900.

van Mierlo, C. P. M., Darby, N. J., Keeler, J., Neuhaus, D., & Creighton, T. E. (1993) *J. Mol. Biol. 229*, 1125−1146.

Wagner, G., Hyberts, S., & Peng, J. W. (1993) in *NMR of Proteins* (Clore, G. M., & Gronenborn, A. M., Eds.) pp 220−257, The Macmillan Press, London.

Wittekind, M., Mapelli, C., Farmer, B. T., II, Suen, K.-L., Goldfarb, V., Tsao, J., Lavoie, T., Barbacid, M., Meyers, C. A., & Mueller, L. (1994) *Biochemistry 33*, 13531−13539.

Yu, H., Rosen, M. K., Shin, T. B., Seidel-Dugan, C., Brugge, J. S., & Schreiber, S. L. (1992) *Science 258*, 1665−1668.

Yuzawa, S., Yokochi, M., Tsuchiya, S., Teresawa, H., Kohda, D., Schlessinger, J., Miura, K., & Inagaki, F. (1996) NMR analysis of a modular protein: Case study of Grb2, Proceedings of the XVIIth International Conference on Magnetic Resonance in Biological Systems, Keystone, Colorado, August 18−23, 1996.

Zhang, O., & Forman-Kay, J. D. (1995) *Biochemistry 34*, 6784−6794.

Zhang, O., & Forman-Kay, J. D. (1996) *Biochemistry* (submitted for publication).

Zhang, O., Kay, L. E., Olivier, J. P., & Forman-Kay, J. D. (1994) *J. Biomol. NMR. 4*, 845−858.

Zhang, O., Forman-Kay, J. D., Shortle, D., & Kay, L. E. (1996) *J. Biomol. NMR* (in press).

BI962548H